



**HAL**  
open science

## Flexible micro-assembly system equipped with an automated tool changer.

Cédric Clévy, Arnaud Hubert, Nicolas Chaillet

► **To cite this version:**

Cédric Clévy, Arnaud Hubert, Nicolas Chaillet. Flexible micro-assembly system equipped with an automated tool changer.. *Journal of Micro-Nano Mechatronics*, 2008, 4 (1), pp.59-72. 10.1007/s12213-008-0012-z . hal-00326611

**HAL Id: hal-00326611**

**<https://hal.science/hal-00326611v1>**

Submitted on 3 Oct 2008

**HAL** is a multi-disciplinary open access archive for the deposit and dissemination of scientific research documents, whether they are published or not. The documents may come from teaching and research institutions in France or abroad, or from public or private research centers.

L'archive ouverte pluridisciplinaire **HAL**, est destinée au dépôt et à la diffusion de documents scientifiques de niveau recherche, publiés ou non, émanant des établissements d'enseignement et de recherche français ou étrangers, des laboratoires publics ou privés.

# Flexible Micro-Assembly System Equipped with an Automated Tool Changer

Cédric Clévy, Arnaud Hubert and Nicolas Chaillet

**Abstract**—This paper deals with the design, fabrication and experimental validation of several modules of a micro-assembly system. On one hand, a microgripper is integrated in a four degrees of freedom system. On the other hand, a tool changer is designed. It enables to exchange automatically the tip part of the microgripper and then dedicated tools can be used to achieve specific tasks. The principle of this tool changer relies on a thermal glue whose phase (liquid or solid) is controlled by heat generators. This system is based on the modeling of thermal phenomena in the tools during a cycle of tool exchange. A compliant system is added to limit micromanipulation forces applied during assembly tasks like insertions. Finally, the successful assembly of several microcomponents is detailed, highlighting the capabilities and benefits of the whole system.

**Index Terms**—Micro-assembly, micromanipulation, microgripper, tool changer, automation.

## I. INTRODUCTION

MICROMANIPULATION and micro-assembly devices have been extensively studied by the scientific community over the last ten years [1]. These devices are used to manipulate micrometric sized components i.e. between 1  $\mu\text{m}$  to 1 mm in different fields such as the assembly of micromechanisms [2] [3], laser sources, optical benches [4] [5] and the manipulation of biology cells or cosmetic powders. Its field of applications is wide because it includes micromechanics as well as micro-optics, microsystems, micro-electronics, but also medicine, biology and pharmacy.

The manipulation of components is widely different if we consider micrometric, milli or centimetric sized components [6] [7]. First of all, the effects of surface forces become predominant [8]. Numerous researches are being performed to understand, model and control these forces [9] [10]. Secondly, in many cases, the weakness of these micro-objects is an important parameter (small size, specific materials used). Consequently, the applied forces during their manipulation must be limited. Finally, for micromanipulation it is required to use high resolution visualization systems (cameras, optical microscopes, Scanning Electron Microscopes) which drastically restrict the manipulation area.

Micromanipulation and micro-assembly tasks are today mainly performed either manually or with highly dedicated machines. Manual assembly causes quality issues, part loss and requires several months of training for unskilled operators. Conversely, using dedicated machines applies on bigger series

C. Clévy, A. Hubert and N. Chaillet are with the AS2M (Department of Automatic Control and Micro-Mechatronic Systems), FEMTO-ST Institute, CNRS 6174 / UFC / ENSMM / UTBM, 24 rue Alain Savary, 25000 Besançon, France. e-mail: cclevy@femto-st.fr.

Manuscript Submitted October 12 2007.

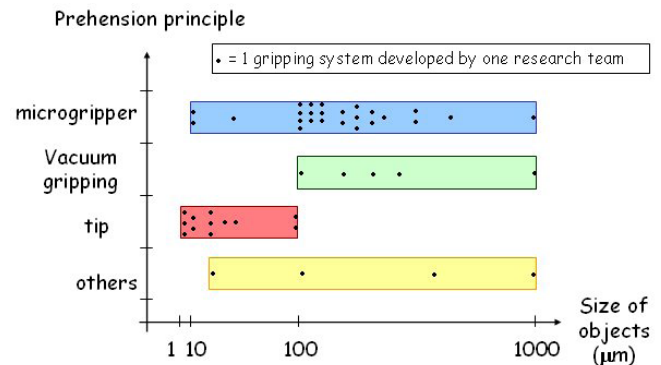


Fig. 1. Synthesis of prehension principles used to manipulate micro-objects. Scale bars represent the working range of the considered gripping principle.

of products because they are expensive and huge (complexity and energy consuming) compared to the size of the final product. Due to these limitations, it is presently very expensive to assemble microproducts [11]. The goal of the works presented in this paper is to assemble small to medium batches of microproducts. It leads to the design of flexible, reconfigurable and automated assembly systems able to perform cheap and constant quality tasks.

To reach this goal, the next section deals with the design and fabrication of a micro-assembly system comprising of a four degrees of freedom device, a workplane and a microgripper. A system to exchange the tip part of the microgripper is then introduced: its design and fabrication are presented in section three whereas the control of this system is presented in section four. The fifth section deals with the design, fabrication and test of a compliant table used to limit micromanipulation forces applied during insertion operations. In the last section, the assembly of several microcomponents is presented to validate experimentally the principles of the complete system.

## II. DESIGN AND FABRICATION OF THE MICRO-ASSEMBLY SYSTEM

In order to develop a new micro-assembly system, it is first necessary to choose the gripping principle. Numerous and various systems already exist. The analysis of the main systems presented in the literature (i.e. microgrippers, needles taking advantage of adhesion forces, vacuum grippers and other ice grippers or microshovel) enables to define the limitations for each gripping principle (Fig. 1 is a compilation of the literature concerning this topic from 1997 to 2007).

Microgrippers are mainly limited by adhesion forces that reduce the success rate of the release. Vacuum gripping, is lim-

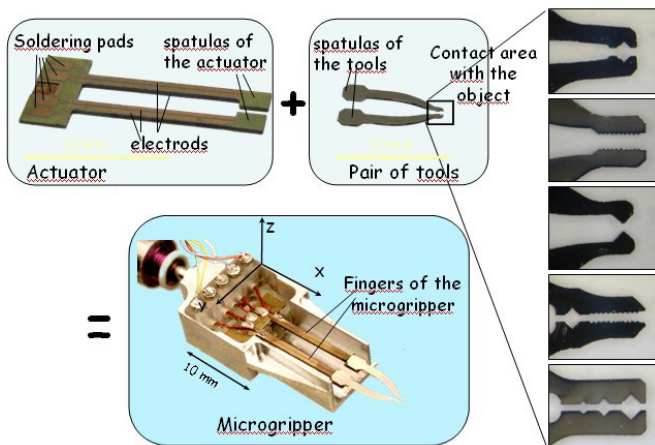


Fig. 2. Design of the microgripper: a suitable pair of tools is fastened at the tip part of a piezoelectric actuator. This set, once packaged constitutes the microgripper.

ited to objects generally bigger than  $100 \mu\text{m}$ . Finally, needle tips require a very good knowledge on adhesion forces. That is why, they do not allow an easy control of the manipulation task (pick and place). They also do not allow the manipulation of objects bigger than  $100 \mu\text{m}$ .

As a conclusion, we chose to use a microgripper. Indeed, it is the less limited gripping system, enabling a good control of the pick and transport tasks. The release can be sufficiently well controlled by using a suitable design of the gripping tools.

The built microgripper is made of two piezoelectric beams (each of them measures  $15 \times 2 \times 0,4 \text{ mm}^3$ ). These beams are powered through a high voltage amplifier. At the tip part of these beams are fastened either irreversible or reversible tools (Fig. 2) [12] [13], temporarily in contact with the manipulated object (see section III). They are passive (Nickel made) and their dimensions are  $10 \times 1 \times 0,18 \text{ mm}^3$ . Different kinds of pairs of tools are available. They are chosen accordingly with two criteria:

- the control of the holding phase: the shape of the tool depends on the size, shape and material of the object to manipulate,
- the control of object's release phase: both the shape minimizing the contact area between tool and object and the roughness are greatly influent.

This microgripper is fastened on a three degrees of freedom micropositioning system (Fig. 3). This system is made of translational stages by Physik Instrumente GmbH. They enable 25 mm of stroke with a unidirectional repeatability of  $0,1 \mu\text{m}$  and a bidirectional backlash of  $2 \mu\text{m}$ . The work plane, i.e. the plane where micro-objects to manipulate are placed, is assembled on a rotational stage enabling rotations of  $360^\circ$ . The whole system is then comprised of a four degrees of freedom device. A TIMM-400C camera from SPI GmbH equipped with a high magnification microscope is used (orientation of  $45^\circ$  with the gripper) in order to get a visual feedback. Finally, the whole system is controlled through a joystick and a computer software (Borland Builder C++ based).

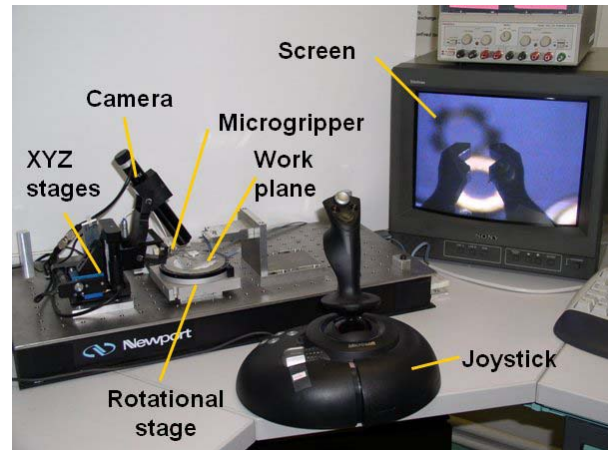


Fig. 3. Large view of the micromanipulation system: it is made of a microgripper fastened on a XYZ structure. The working plane is assembled on a rotational axis. A camera displays visual feedback. The whole system is driven through a joystick and a computer.

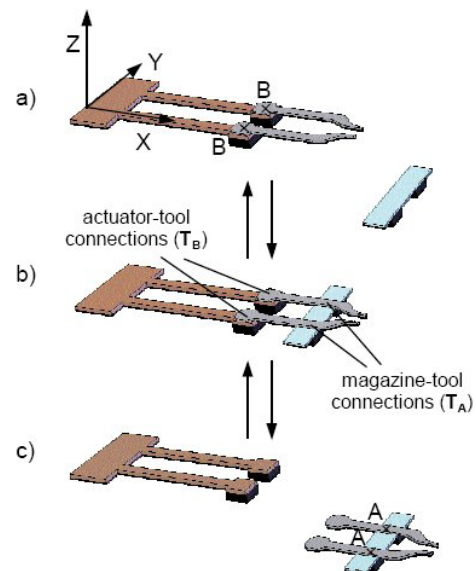


Fig. 4. Phases of a tool exchange: (a) a pair of tools is fastened on the tip part of the actuator of the microgripper - (b) the pair of tools is fastened on the tip part of the gripper and in the meantime on the magazine - (c) the pair of tools is fastened on the magazine. The exchange of a pair of tools is done by the succession of steps a-b-c-b-a.

### III. DESIGN AND FABRICATION OF THE A TOOL CHANGER FOR MICROGRIPPER

#### A. General Design

The micromanipulation system described in the previous section is not flexible enough to complete micro-assembly. Indeed, it is only made of one gripping system, and its characteristics does not allow the manipulation of a wide range of objects (the stroke of the gripper is  $320 \mu\text{m}$  for  $\pm 100\text{V}$  applied, the shape of the pair of tools is dedicated). To enable the successive manipulation of various objects, it is required to use successively the suitable pair of tools. Until now, few multitools systems adapted to microrobotic requirements have been developed. They consist in exchanging the whole

gripping system (gripper changer or tool rotators) [14] [15] but they require either large strokes or large free space and offer a limited choice of tools and also requires electrical connections. For reasons of available free space, precision, electrical connections and alternative technical solutions, we chose to design a system allowing to exchange only the tools of the microgripper [16]. The principle of this tool changer consists in temporarily fastening one pair of tool either at the tip part of the actuator (points B, Fig. 4) of the microgripper or in a magazine (points A, Fig. 4).

### B. Selection of a temporarily fastening principle

Technically, several solutions can be used to temporarily fasten the pair of tools either at the tip part of the actuator of the microgripper or in the magazine. The five main solutions are the following ones:

- solutions based on mechanical bending,
- electromagnetic solutions,
- electrostatics solutions,
- solutions based on reversible polymers and glues,
- solutions based on van der Waals forces.

Several systems, like clamped connections, able to connect mechanically two microparts together have already been designed [17] [2]. They generally consist in two bending beams with a small hook at their tip. The part to clamp is then inserted in a hole. Such systems take advantages of recent progress of microfabrication processes. Nevertheless, few of them are reversible in the sense that the clamped part can be removed [18] [19]. The weak point of temporarily mechanical fastening systems is that the material wear reduces their performances (positioning accuracy, forces transmitted and automation).

Electromagnetic effects are favored by scale decreases for magnets and also for microcoils [20]. Let us consider an interaction between two magnets (numbered 1 and 2). The magnetic energy  $E_{mag}$  of the magnet n° 2 resulting from the interaction between magnet n° 1 and magnet n° 2 can be written as follows:

$$E_{mag} = - \int \mu_0 \cdot \vec{M}_2 \cdot \vec{H}_1 dV \quad (1)$$

with  $\vec{M}_2$  the magnetization of magnet 2 and  $\vec{H}_1$  the magnetic field generated by the magnet 1 at the position of magnet 2. The force  $\vec{F}_{12}$  exerted by magnet 1 on magnet 2 results from the variation of this energy regarding to the position of magnet 2:

$$\vec{F}_{12} = \frac{\partial E_{mag}}{\partial \vec{r}} = \overrightarrow{grad}(E_{mag}) \quad (2)$$

These equations point out that an homothetic reduction of all the dimensions (dimensions and distance between them) of a magnetic dipole by a factor of 10 (i.e. its volume is divided by a factor of 1000) causes a reduction of the magnetic force by a factor of 100. Thus, the weight to force ratio  $P/F_{12}$ , where  $P$  is the weight of magnet 2, is multiplied by 10, making magnets particularly interesting for small size systems.

For an interaction between a coil and a magnet, the weight to force ratio remains unchanged. For an interaction between

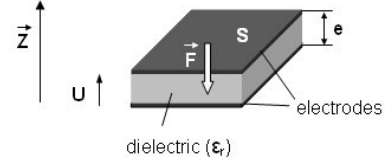


Fig. 5. Scheme of a plane capacitor, a force  $F$  results from the application of a voltage  $U$ .

two coils, this force decreases. Nevertheless, current densities applied to coils, are usually limited to  $5 \text{ A/mm}^2$  (at the macro scale), whereas at the micro scale, this limit can be extended to thousands of Amperes by square millimeter [20]. This is due to the thermal conduction and convection that are much favored at the micro scale (surface/volume ratio increases while scaling down) [21]. The conclusion is that all the electromagnetic configurations are favored by a reduction of size, generating important blocking forces. The weak point of such systems is that they can disturb, at distance, the behavior of the manipulated object (magnetization for instance).

Scaling down is favorable to electrostatic based temporarily fastening systems. Let us consider a capacitor built with two parallel electrodes (surface  $S$ ). A voltage  $U$  is applied between both electrodes. The energy stored is:

$$E_{elec} = \frac{C \cdot U^2}{2} \quad \text{with} \quad C = \epsilon_r \cdot \epsilon_o \cdot \frac{S}{e} \quad (3)$$

Where  $C$  is the capacity of the capacitor,  $\epsilon_r$  the dielectric permittivity ( $\epsilon_r = 1$  for air),  $\epsilon_o$  is the vacuum permittivity ( $\epsilon_o = 8,85 \cdot 10^{-12} \text{ s}^4 \text{ A}^2 / \text{m}^3 \text{ kg}$ ) and  $e$  the dielectric thickness between the two electrodes. The attraction force  $F$  between electrodes is computed from its virtual work:

$$F = \frac{\partial E_{elec}}{\partial e} = \frac{\epsilon_o \cdot \epsilon_r \cdot U^2 \cdot S}{2 \cdot e^2} \quad (4)$$

In addition, electrostatic forces decrease less than gravity forces in direct ratio. Moreover, microfabrication techniques are particularly well adapted to the fabrication of such systems. Nevertheless, uncontrolled effects caused by electrostatic fields can be damaging on manipulated objects.

It is also possible to design a temporarily fastening system based on the use of polymers and glues. Solutions using scotch<sup>®</sup> (double-faced), post-it<sup>®</sup>, gel-pack<sup>®</sup> (currently used to hold small samples in their packaging) or PDMS (PolyDiMethlySiloxane) enable a very simple design of a temporarily fastening system. Nevertheless it has been proven that the intensity of blocking forces between both assembled parts varies a lot with the number of experiments, in the range of several hundreds of per cent. Dust also affects a lot the performances of such a system [22].

Thermal glues can also be considered. Their phase (i.e. solid or liquid) depends on temperature. They can successively become solid (at room temperature) and liquid (temperature in the order of 60 to  $100^\circ \text{ C}$  depending on the glue used) during hundreds of cycles with a good reliability [23]. This solution enables a good transmission of the forces and the heating

is extremely short during a cycle reducing the drawback of heating the whole system.

Finally, van der Waals forces, even if they act at a distance lower than 100 nm, can be exploited to develop a temporarily fastening system. For example let us consider the works of several groups who developed biomimetic materials based on the same principle that the one used by Gecko lizards to walk on the walls [24]. This system consists in very small hair with a 100 to 200 nm spatulas at the tip of each of them. First experiments shown good results excepted a great fragility and short life time (due to dust particles in air).

Solutions	Mech.	ElectroM.	ElectroS.	Th. Glues	VdW
Reliability	-	+++	+	+++	+
Force transmitted	+++	+++	+	+++	+
Reversibility	+	+++	+++	+++	-
Automation	+	+	+	+	-
Perturbations at a distance	+++	-	-	+	+++

TABLE I

COMPARISON OF SOLUTIONS FOR TEMPORARILY FASTENING MICRO-OBJECTS. MECH., ELECTROM., ELECTROS., TH. GLUES AND VdW RESPECTIVELY REFER TO SOLUTIONS BASED ON MECHANICAL BENDING, ELECTROMECHANICAL, ELECTROSTATICS, THERMAL GLUES AND VAN DER WAALS FORCES. THE "+" CORRESPONDS TO A POSITIVE EVALUATION AND THE MARKS GO FROM "-" TO "+++".

Theses arguments allowed to compare all these solutions using criteria that directly depend on the application required (temporarily fastening system for designing a tool changer for microgripper). The main ones are the reliability, force transmitted, reversibility, automation and influence at a distance on manipulated objects. Table I displays qualitative results. In this table, each solution is evaluated for the whole criteria. As an example and considering arguments previously detailed above, electromechanical, electrostatic and thermal glue based systems are very favorable to design a reversible system (+++ mark), whereas mechanical bending systems suffer from wear and difficulties of design a reversible system (+ mark because despite difficulties, this kind of solution seems possible). Finally, designing a reversible van Der Waals forces based system does not appear as a viable solution today (- mark).

The use of a thermal glue with low melting point ( $62^{\circ}\text{C}$ ) obtains the best marks. It appears as a simple and original solution and is open to meet most of the required criteria.

### C. Design of the thermal glue based tool changer

As mentioned in the previous section, a thermal glue is used to enable the temporarily fastening of a pair of tools either at the tip part of the actuator of the microgripper or in the magazine. Several thermal glues are available, but we chose the one commercially available with the lowest melting point temperature i.e.  $62^{\circ}\text{C}$ . The whole cycle of the glue is described on Fig. 6.

To generate the phases changes of the glue, it is required to use heating elements. After a comparison of several solutions (Peltier stacks, small resistors and 2D microfabricated heaters), it was chosen to use small Surface Mounted Devices (SMD)  $6\ \Omega$  resistors ( $2 \times 1.25 \times 0.45\ \text{mm}^3$ ). These resistors are placed

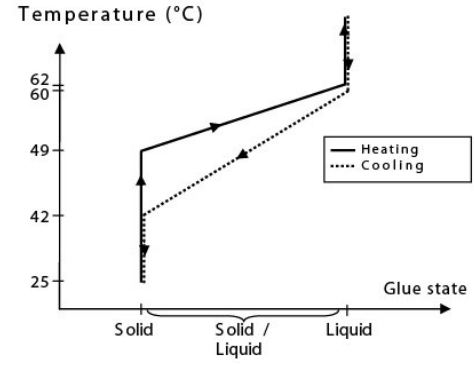


Fig. 6. Phase of the thermal glue during a whole cycle of heating and cooling.

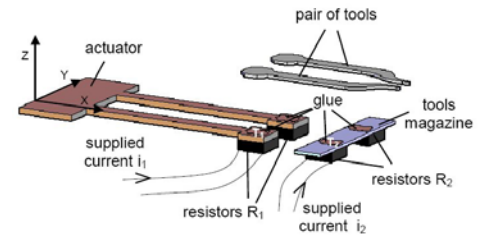


Fig. 7. Scheme of the set actuator-tools-resistors-magazine. The glue is deposited at the contact between the tip of the actuator and the tools (2 points) and also between the tools and the magazine (2 points).

under each contact where a temporarily fastening is required (Fig. 7). The suitable power of each resistor has to be chosen to generate either the liquefaction of the glue at the considered contact (resistors powered on, generating heat) or the solidification of the glue (resistors switched off, stopping the heating then becoming cold due to conduction and convection exchanges).

## IV. CONTROL OF THE TOOL CHANGER FOR AUTOMATIC WORKING

### A. Objective

In order to achieve efficient tool exchanges (shorter cycle time, best positioning accuracy), it is required to study precisely the power dissipated inside the resistors versus the time evolution. Indeed, let us consider the situation b) from Fig. 4. This configuration is the initial one, from which the two following configurations are possible:

- heating both resistors at the contacts between tools and magazine (points A). This leads to the configuration of micromanipulation (situation a) from Fig. 4) where the glue at contacts A must be liquid while in the meantime, the glue at contacts B must remain solid to ensure a good positioning,
- heating both resistors at the contacts between tools and actuator (points B). This leads to the configuration of tool exchange because the pair of tools is unloaded in the magazine (situation c) from Fig. 4) where the glue at contacts B must be liquid while in the meantime, the glue at contacts A must remain solid.



Situation b) is delicate because the heating of resistors at the A contacts, generates a heating of the Nickel tools (conduction). This heating of the tools generates the unwanted heating of the glue at contacts B. In the same way, the heating of contacts B generates an unwanted heating of contacts A. In order to reduce this unwanted effect, it is required to control precisely the input signal of the different resistors. The intensity of the power and its duration are the main key points.

The solution consists in an open loop control because closed loop control requires sensors (problems of free space, precision of positioning and electrical connections). To ensure the requirements with open loop control, a study of thermal phenomena in a tool from situation b) depicted in Fig. 4 is developed. This study consists firstly in the modeling of thermal phenomena, and secondly in the identification of all the parameters which affect this model. This model will then be used to define the control laws of the resistors during a cycle of tool exchange. Finally the performances of the system will be experienced.

### B. Modeling

The modeling of thermal phenomena in the tools relies on the energy conservation law [25]:

$$\int_V \rho \cdot C \cdot \frac{\partial T}{\partial t} dV = - \int_S \vec{q} \cdot \vec{n}_{ext} dS + \int_V Q dV \quad (5)$$

where  $\rho$  is the mass density,  $C$ , the calorific capacity,  $V$  the volume of the considered element,  $S$  the surface of the considered element,  $\vec{q}$  the heat flux density and  $Q$  the volumic heating source. In this study, thermal radiation is neglected. Thermal heat flux density includes conduction and convection:

$$\vec{q} = \vec{q}_{cond} + \vec{q}_{conv} \quad (6)$$

with :

$$\begin{cases} \vec{q}_{cond} = -\lambda \cdot \vec{\nabla} T & \text{(Fourrier's law)} \\ \vec{q}_{conv} = h \cdot (T - T_\infty) \cdot \vec{n}_{ext} & \text{(Conducto-convective approximation)} \end{cases} \quad (7)$$

where  $\lambda$  is the conduction coefficient of the considered element,  $h$  the convection coefficient at the surface of the element and  $T_\infty$  the ambient temperature. Because of the thickness of the tools (180  $\mu\text{m}$ ), the temperature will be considered constant in a cross-section. The modeling appears now as a one dimensional problem along the X axis. This hypothesis leads to the following local equation where T is a function of space and time,  $T = T(x,t)$ :

$$\rho \cdot C \cdot \frac{\partial T}{\partial t} = \frac{\partial}{\partial x} \left[ \lambda \cdot \frac{\partial T}{\partial x} \right] - \tilde{h} \cdot (T - T_\infty) + Q \quad (8)$$

$\tilde{h} = 2 \cdot \frac{(w+e) \cdot h}{w \cdot e}$  with  $w$  and  $e$  that are respectively the width and thickness of the considered element. The volumetric heating source  $Q$  is distributed along the X axis, then, it is considered that in the tool  $Q = 0$  and in the resistor  $Q = \frac{R \cdot I^2}{V_R}$ , with  $R$  the value of the resistor,  $I$  the feeding current and  $V_R$  its volume. Materials (actuator, tools, resistors, magazine), glue, shapes, wires, contacts have an effect upon thermal phenomena. In order to define the control laws of

the resistors, a simplified model has been used as a first step neglecting the influence of the actuator and magazine. The influence of this strong hypothesis will be verified later.

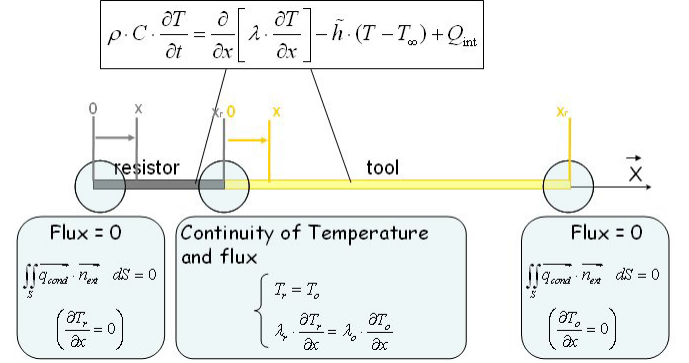


Fig. 8. 1D modeling scheme and hypothesis.

Thus, the used model is schematized on Fig. 8 (subscript  $r$  corresponds to the resistor and subscript  $o$  corresponds to the tool):

- the simplified model is made of a resistor part at the tip of which is connected a tool part,
- the boundary conditions are: no flux is considered at the extremity of both constituents,
- the continuity conditions are: temperature and flux are considered to be continuous between the resistor and tool.

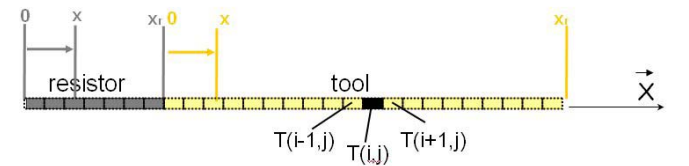


Fig. 9. Meshing and elements used in the modeling at time  $j$ .

Several modeling techniques were used, among them a FEM model built using Comsol-multiphysics, an analytical model which requires the use of a Green function and a numerical model. For complexity reasons and comparison between results of the models and experiments, a numerical model based on a finite difference method was chosen. It gives a recurrent equation from the local equation (8). The temperature  $T(x,t)$  is then approximated by the series  $T(i,j)$  with  $i$  the index of space sampling and  $j$  the index of time sampling (See Fig. 9). First order derivative was approximated by an Euler numerical scheme and second order derivative with a control difference schema [26]. After calculations, the

recurrent equation can be written as follows:

$$\begin{aligned}
T(i, j+1) = & \frac{\lambda(i+1)}{(\Delta x)^2} \cdot \frac{\Delta t}{\rho(i) \cdot C(i)} \cdot T(i+1, j) \\
& + \left(1 - \frac{\lambda(i+1) + \lambda(i)}{(\Delta x)^2} \cdot \frac{\Delta t}{\rho(i) \cdot C(i)}\right. \\
& \quad \left. - \widetilde{h}(i) \cdot \frac{\Delta t}{\rho(i) \cdot C(i)}\right) \cdot T(i, j) \\
& + \frac{\lambda(i)}{(\Delta x)^2} \cdot \frac{\Delta t}{\rho(i) \cdot C(i)} \cdot T(i-1, j) \\
& + \widetilde{h}(i) \cdot \frac{\Delta t}{\rho(i) \cdot C(i)} \cdot T_\infty + \frac{\Delta t}{\rho(i) \cdot C(i)} \cdot Q(i) \quad (9)
\end{aligned}$$

This equation can be written as a state space model where the state ( $\mathbf{X}(j)$ ) contains the temperature of all elements at time  $j \cdot \Delta t$ , ( $\mathbf{X}(j) = \{T(1, j) \cdots T(N, j)\}^T$ ):

$$\begin{cases} \mathbf{X}(j+1) = \mathbf{A} \cdot \mathbf{X}(j) + \mathbf{B} \cdot \mathbf{U}(j) \\ \mathbf{Y}(j) = \mathbf{C} \cdot \mathbf{X}(j) + \mathbf{D} \cdot \mathbf{U}(j) \end{cases} \quad (10)$$

$\mathbf{U}$  is the command of the system composed with the thermal source at each point and the ambient temperature  $\mathbf{U}(j) = \{Q(1, j) \cdots Q(N, j) T_\infty\}^T$ . Finally,  $\mathbf{A}$  is the state matrix based on the recurrent equation (9) and from the boundary conditions. The details of the  $\mathbf{A}$  matrix are not reported in this paper because of its complexity and size.  $\mathbf{C}$  is the matrix which depends on the temperature locations considered as output. The  $\mathbf{D}$  matrix is null in our case. With the state space model, the temperature in each element at any time can be defined as a function of the current supplied in the resistor and initial state.

### C. Identification

Symbol	Parameter	Value	Unit
$h_r$	convection coeff. of the resistor	35.3	$W/m^2K$
$h_o$	convection coeff. of the tool	38	$W/m^2K$
$\lambda_r$	conduction coeff. of the resistor	90.	$W/mK$
$\lambda_o$	conduction coeff. of the tool	49.3	$W/mK$
$\rho_r$	mass density of the resistor	2520	$kg/m^3$
$\rho_o$	mass density of the tool	8900	$kg/m^3$
$C_r$	calorific capacity of the resistor	790	$J/K.kg$
$C_o$	calorific capacity of the tool	765	$J/K.kg$

TABLE II  
NUMERICAL VALUES OBTAINED AFTER IDENTIFICATION.

The state space equations presented in the previous section contain parameters such as the conductivity and convection coefficients of the tool and resistor. The value of the coefficients in the equations have to be known. Because the material properties of the tool and resistors are not well and precisely known, an identification step is required. Several methods were experienced. The one that gives the best results consists in using a steady state analytical solution. Details are available in [27]. This procedure requires thermocouples to measure the temperature evolution versus time for several points along the tool. These thermocouples were only used for the identification step. Their influence is supposed to be negligible due to their small diameter (25  $\mu m$ ) compared with the section of the tools

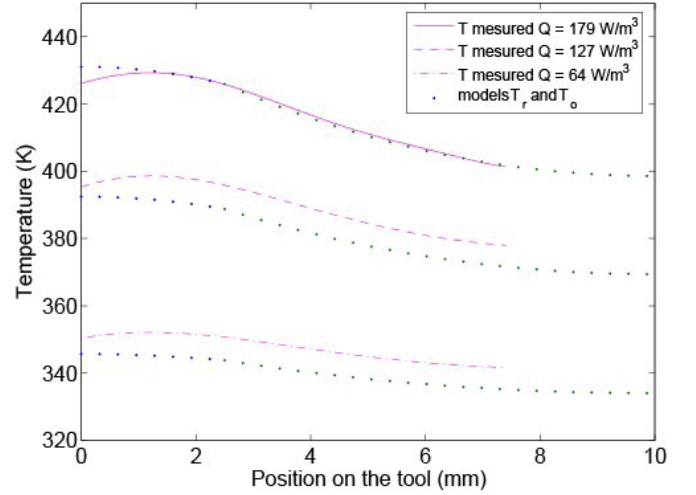


Fig. 10. Comparison between steady state simulation and experimental measurements for three heat sources ( $Q = 179W/m^3$  was used for the identification whereas  $Q = 127W/m^3$  and  $Q = 64W/m^3$  were used to check the validity of the results).

( $1 \times 0.18 \text{ mm}^2$ ). The identification procedure was performed for  $Q = 179W/m^3$ . The results obtained are detailed in Tab. II.

In order to validate all the hypothesis taken during the modeling, several experiments were performed. The first one consists in determining the accuracy of the model for the steady state behavior. For this experiment, a thermocouple carried by a microprecision translation stage was used to measure the temperature of the steady state along the tool. Fig. 10 displays these results showing a good correlation between modeling and experiments.

The second experiment consists in comparing the simulation results to experimental measurements for the transient behavior. For this experiment, two thermocouples were used at the same time, one to measure the temperature at the point A and the second at the point B. These comparisons allow the validation of some hypotheses such as the fact that thermal radiation can be neglected. Fig. 11 displays the results obtained showing a good correlation between modeling and experiments.

### D. Control laws

One of the objectives of the modeling consists in defining the control laws of the tool changer resistors. In that way, two requirements have to be checked:

- the liquefaction of the glue at the contact surface between actuator and tool, respectively tool and magazine, must be total, i.e. over than  $62^\circ C$ ,
- the difference of temperature between both contacts must be as most important as possible. Temperature at the contact between tool and magazine, respectively between actuator and tool, must be lower than  $49^\circ C$  to guarantee the solid phase of the glue.

Considering these two requirements, the numerical model was used to define the control laws of the resistors during a cycle of tool exchange. Fig. 12 displays the chronograms

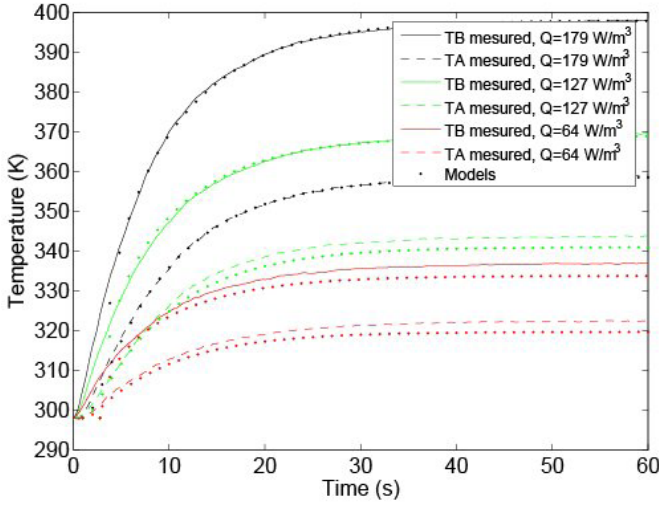


Fig. 11. Comparison between transient part of simulations and experimental measurements for three heat sources ( $Q = 179 \text{ W/m}^3$  was used for the identification whereas  $Q = 127 \text{ W/m}^3$  and  $Q = 64 \text{ W/m}^3$  were used to check the validity of the results).

of the power dissipated inside the resistors at the contact tool-actuator (R1) and at the contact tool-magazine (R2). The numbers indicate the different phases of the tool exchange cycle. Initially, the tools are fastened both at the actuator and magazine:

- 1 - heating of resistors R2, breaking the fastening between tool and magazine,
- 2 - micromanipulation step (the tools are only fastened at the tip part of the actuator),
- 3 - heating of resistors R2 generating the liquefaction of the glue at the contact between tool and magazine,
- 4 - fastening of this pair of tools in the magazine,
- 5 - heating of resistors R1 breaking the fastening at the actuator-tool contact,
- 6 - motions of the actuator alone reaching the position of a second pair of tools,
- 7 - heating of resistors R1 generating the liquefaction at the actuator-tool contact,
- 8 - fastening of this second pair of tools both at the actuator and magazine.

It must be pointed out that the temperature variation due to the heating of phases 3 and 7 are not taken into account for several reasons: first, for phase 3, a pair of tools is initially only fastened at the actuator, so the corresponding position of the magazine is free, its resistors are cold. Secondly, resistors R2 are switched on causing the heating of the corresponding position in the magazine. Third, once the heating finished, the tools are placed at the corresponding contact in the magazine, the solidification time is short and difficult to model. Phase 7 happens in the same way that the phase 3.

### E. Performances

Using these results, several experiments were performed to define the performances of the tool changer. First of all, hundreds of successive tool exchanges were done

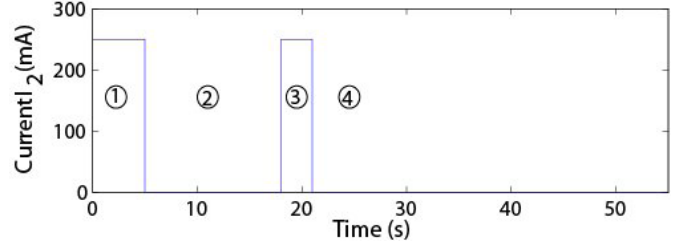
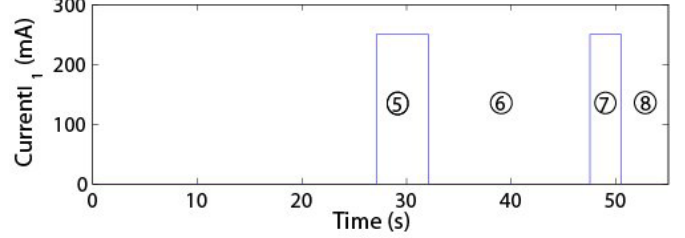
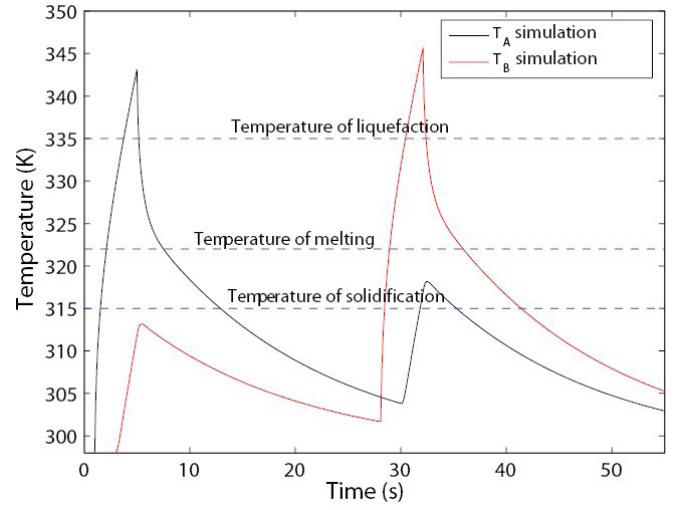


Fig. 12. Example of the temperatures evolution versus time of resistors at the contact between actuator and tools (R1) and at the contact between tools and magazine (R2) when respectively powered by  $I_1$  and  $I_2$  currents. These values results from the numerical model and do not take into account phases 3 and 7.

automatically without adding glue. These automatic cycles enable to measure the tools positioning accuracy. In this aim the initial position of a tool is measured, the tool is then unloaded in the magazine, and after a while it is taken out of the magazine and positioned at the same place in front of the sensor. A laser sensor (Keyence) with a resolution of 10 nm was used. X, Y and Z axes are depicted Fig. 7. These experiments shown that the positioning accuracy of the tool is always better than  $3 \mu\text{m}$  (maximal deviation of  $3.2 \mu\text{m}$ ,  $2.3 \mu\text{m}$  and  $2.8 \mu\text{m}$  along X, Y and Z axes respectively) and is of  $1 \mu\text{m}$  in average (average of respectively  $0.74 \mu\text{m}$ ,  $0.62 \mu\text{m}$  and  $0.03 \mu\text{m}$  along the X, Y and Z axes) [28].

Mechanical experiments were also performed. It has been measured that on each finger, a force of 300 mN can be applied at the tip of the tool, along the Y axis, before breaking the glue film. This value is higher than the maximum



micromanipulation force that can be applied by the piezo-actuator (55 mN) [13]. Thus, along the Y axis, the glue film will be strong enough to allow micromanipulation tasks.

Along the Z axis, a force of 27 mN has to be applied to break the glue film. Along this axis the maximum force that can be applied by the actuator is 10 mN. Let us note that 27 mN is less than the mechanical force limit of the actuator itself (trajectory generating a collision for instance). This is a very interesting result because it means that the glue film acts as a fuse along the Z axis which is the direction of insertion.

The tools are initially placed by hand at the tip of the actuator. Then, a precise repositioning has so to be performed before using the tools for a micromanipulation task. This phase requires the relative positioning of the tools. The tool changer allows such a step by driving only one of both resistors of the actuator, or one of both resistors of the magazine. This possibility allows to fasten one tool at the tip of the actuator and the other on the magazine.

An other interesting result is that the tool changer has been experienced successfully in the vacuum chamber of a scanning electron microscope (SEM) despite all the changes (pressure that influence thermal phenomena...). In this aim several experiments were performed, among them the degassing process of the glue during a tool exchange or the temperature of melting, liquefaction and solidification of the glue. There are several important advantages of using the tool changer in the chamber of the SEM:

- the free space is again more limited in the chamber of a SEM (about  $25 \times 25 \times 25 \text{ cm}^3$  compared to about  $40 \times 40 \times 40 \text{ cm}^3$  usually required for in air devices),
- the time to exchange a pair of tools is considerably short (in a range of 1/20) compared to the time to exchange manually the gripper (solution without tool changer) which requires mainly to stop the SEM and open its door.

More details about applications of the tool changer in the SEM are available in [29].

Finally, the tool changer offers a high flexibility to the micro-assembly system and allows to choose the suitable pair of tools accordingly to the micromanipulation task to perform. The magazine that has been designed offers three places for three pairs of tools for an space volume of  $25 \times 22 \times 2 = 1100 \text{ mm}^3$  whereas the useful space volume of one gripper alone is of  $32 \times 13 \times 10 = 4500 \text{ mm}^3$ .

## V. FORCE LIMITATION SYSTEM

### A. Objective

The whole micro-assembly system enables to perform numerous and various micro-assembly tasks as developed in the next section. Nevertheless, these experiments revealed several difficulties for specific tasks such as insertion. Another problem is that gripping forces are not controlled. Interaction forces can either be measured and controlled or limited with a compliant system. Several works have been done to develop

force sensors adapted to micromanipulation needs. Nevertheless, it is still quite difficult to obtain a system which size, resolution and dynamics are compatible with this application [30] [31] [32] [33]. Several other research teams meet this problem, most of them solved it by using a compliant system in order to limit or control the applied forces. Several solutions have been studied. The most used consists in developing microgrippers with a flexible part [34] [35] [36]. Popa et al., for their part developed a compliant system allowing to hold optic fibers during their fastening (with glue) on a support [37]. Another solution consists in fastening the work plane (where the objects to manipulate are placed) on a compliant structure (levitation system in [38]). The special design of our micro-assembly system leads toward this kind of solution. This greatly reduces the danger of breaking fragile parts (manipulated object, tools or actuator of the microgripper), the potential damages caused on micropositioning stages and increases the feasibility of some specific micromanipulation tasks.

### B. Design of a compliant table

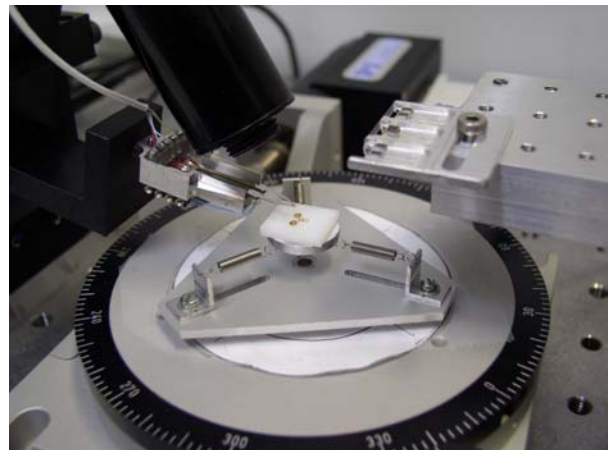


Fig. 13. Close view of the micro-assembly system focused on the compliant table.

The compliant table designed is assembled with a small platform (10 mm of diameter) fastened at the tip of three identical springs guaranteeing smoothness and stability at the same time (Fig. 13). The weak stiffness of the structure, equals to 6.7 N/m (a force of 10 mN along Z generates a motion of 1.5 mm in the same direction), allows to limit the intensity of the forces applied and increases the success rate of some applications like insertion tasks. This system enables to define precisely the time when a contact is established between the gripper and the workplane. The structure of the compliant table was chosen to make it independent from other elements of the micro-assembly system. Thus, it is sometimes possible to put it or to remove it depending on the needs (modularity concept).

## VI. EXPERIMENTATIONS

Using the complete device described in this paper, numerous micromanipulation and micro-assembly tasks were performed with success. The main ones are:

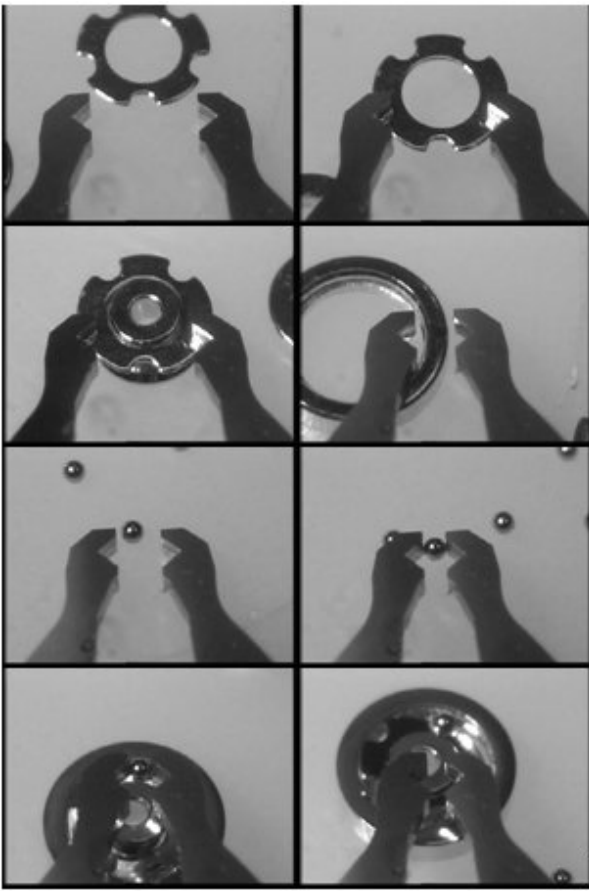


Fig. 14. Assembly sequence of the ball bearing (from top left to bottom right) : the initial gap between the tools is of 1 mm. It enables the manipulation of the cage of the bearing. The gap between the tool is then changed using the tool changer capabilities. The new gap between the tools is of  $200\ \mu\text{m}$  allowing the manipulation of the outer ring of the bearing and the insertion of the five balls (one by one). Thus, the whole assembly of the bearing (except the final crimping) can be performed with the micro-assembly system.

- ball bearing of 1.6 mm in outside diameter including 5 balls of  $200\ \mu\text{m}$  in diameter (a full assembly sequence is displayed by Fig. 14),
- miniature gears for watch industry,
- micromechanisms (a full assembly sequence is displayed by Fig. 15),
- rock grains of  $20\ \mu\text{m}$  in diameter to study the behavior of bacterias at it's contact (biological application),
- insertion of a wire of  $50\ \mu\text{m}$  in diameter in the eye of a needle (hole of  $70\ \mu\text{m}$  in diameter) for opthalmological needs,
- varied grains, spheres of various sizes, shapes and materials,
- tensile samples (length = 1 mm) for mechanical testing at the microscale,
- microscanner,
- various lenses for micro optical components (up to  $125\ \mu\text{m}$  in diameter).

All these experiments demonstrate the usefulness of all the modules of the micro-assembly station and its flexibility.

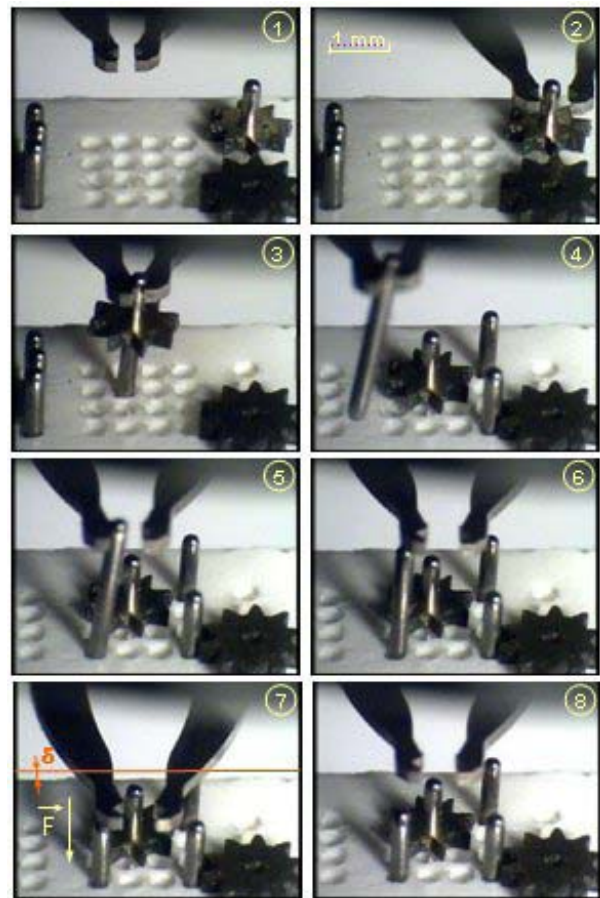


Fig. 15. Assembly sequence of a micromechanism, the diameter of the parts is of  $300\ \mu\text{m}$ , the compliant table is used : (1) initial configuration (2) approach (3) pick and place of the first gear (4) two pins have been manipulated, the third one is picked, positioned but released in the wrong way (5) this wrong positioning makes that the pin cannot be inserted as a standard way (6) the microgripper is used to allow the final insertion of the pin (7) a force along the axis of the pin is applied by the microgripper, the compliant table becomes bent under the applied force (8) once the insertion is a success, the force applied by the microgripper is relaxed.

## VII. CONCLUSION

This paper considers industrial and scientific interests for micro-assembly. Some of these interests lead toward automated assembly systems that are flexible enough to produce small to medium series. Their size is also critical due to assembly accuracy required. In this aim a micro-assembly system has been designed, manufactured and used for several kinds of applications.

First of all, a micromanipulation system comprising of a microgripper, a four degrees of freedom device, driven through a computer has been developed. In order to enable the successive use of dedicated tools to achieve specific tasks, a system of tool changer has been designed and built. It allows to exchange the tip part of the microgripper in an extremely small free space. The principle of this system relies on the use of a thermal glue which phase (i.e. liquid or solid) allows to fasten the pair of tools either at the tip part of the actuator of the microgripper (micromanipulation configuration) or in a magazine (tool exchange configuration). In order to control

precisely the phase of the glue and optimize the working cycle time of the system, thermal effects occurring in the tools have been modeled. Using control laws resulting from these models, hundreds of tool exchanges were performed automatically. The system of tool changer brings a high flexibility to the whole micro-assembly system. It also presents a good positioning accuracy (1  $\mu\text{m}$  in average), allows safe micromanipulation tasks and is compatible with the environment of a scanning electron microscope.

Finally, a compliant table has also been developed to limit the forces applied during the micromanipulation tasks. This system is mainly useful for insertion tasks. Its stiffness of 6.7 N/m improves the efficiency of several kinds of operations.

Future works will mainly concern the automation of the system by integrating vision and force sensing capabilities.

#### ACKNOWLEDGMENT

This work has partially been supported by the European Project ROBOSEM (G1RD-CT2002-00675).

#### REFERENCES

- [1] H. V. Brussel, J. Peirs, D. Reynaerts, A. Delchambre, G. Reinhart, N. Roth, M. Weck, and E. Zussman, "Assembly of microsystems," *Annals of the CIRP*, vol. 49, no. 2, pp. 451–472, 2000.
- [2] K. Tsui, A. A. Geisberger, M. Ellis, and G. Skidmore, "Micromachined end-effector and techniques for directed mems assembly," *Journal of Micromechanics and Microengineering*, vol. 14, pp. 542–549, 2004.
- [3] N. Dechev, J. K. Mills, and W. L. Cleghorn, "Mechanical fastener designs for use in the microassembly of 3d microstructures," in *IMECE, ASME International mechanical engineering congress and RID expo*, 2004.
- [4] D. Popa, R. Murthy, M. Mittal, J. Sin, and H. Stephanou, "M3-modular multi-scale assembly system for mems packaging," in *IEEE/RSJ International Conference on Intelligent Robots and Systems*, Beijing, China, 2006, pp. 3712–17.
- [5] T. Udeshi and K. Tsui, "Assembly sequence planning for automated micro assembly," in *International Symposium on Assembly and Task Planning*, 2005.
- [6] A. Menciassi, A. Eisenberg, I. Izzo, and P. Dario, "From "macro" to "micro" manipulations: models and experiments," *ASME/IEEE Transaction on Mechatronics*, vol. 9, no. 2, pp. 311–319, 2004.
- [7] A. Bourjault and N. Chaillet, *La microrobotique*, Lavoisier, Ed. Hermes, 2002.
- [8] R. S. Fearing, "Survey of sticking effects for micro parts handling," in *International workshop on Intelligent Robots and Systems*, Pittsburg, USA, 1995.
- [9] P. Rougeot, S. Régnier, and N. Chaillet, "Forces analysis for micro-manipulation," in *CIRA*, Espoo, Finland, June 2005.
- [10] P. Lambert and A. Delchambre, "Design rules for a capillary gripper in microassembly," in *International Symposium on Assembly and Task Planning*, Montréal, Canada, July 2005.
- [11] J. J. Koelemeijer Chollet, S., "Cost efficient assembly of microsystems," *MST-News*, 1999.
- [12] J. Agnus, "Contribution à la micromanipulation : étude, réalisation, caractérisation et commande d'une micropince piézoélectrique," Ph.D. dissertation, Université de Franche-Comté, 2003.
- [13] J. Agnus, P. D. Lit, C. Clévy, and N. Chaillet, "Description and performances of a four-degrees-of-freedom piezoelectric microgripper," in *International Symposium on Assembly and Task Planning*, 2003, pp. 66–71.
- [14] B. Winzek, S. Schmitz, and T. Sterzl, "Microgrippers with shape memory thin film actuators," in *IPAS*, Bad Hofgastein, Austria, February 2004, pp. 77–84.
- [15] M. Weck and C. Peschke, "Assembling hybrid microsystems," October 2003, iAP Workshop-Advanced Mechatronic Systems-Lovain la Neuve.
- [16] C. Clévy, "Contribution la micromanipulation robotisée : un système de changement d'outils automatique pour le micro-assemblage," Ph.D. dissertation, Université de Franche-Comté, 2005.
- [17] N. Dechev, W. L. Cleghorn, and J. K. Mills, "Construction of a 3d mems microcoil using sequential robotic microassembly operations," in *ASME International Mechanical Engineering Congress and R&D expo*, Washington D.C., USA, November 2003.
- [18] G. D. Skidmore, M. Ellis, E. Parker, N. Sarkar, and R. Merkle, "Micro assembly for top down nanotechnology," in *International symposium on Mechatronics and human science*, Nagoya, Japan, 2000, pp. 3–9.
- [19] C. Clévy, A. Hubert, and N. Chaillet, "Temporary fixing systems for applications in microrobotics," in *4th IFAC Symposium on Mechatronic Systems*, Heidelberg, Germany, 2006.
- [20] O. Cugat, *Micro-actionneurs électromagnétiques MAGMAS*, Lavoisier, Ed. Hermes, 2002.
- [21] J. Peirs, "Design of micromechatronic systems: scalelaws, technologies, and medical applications," Ph.D. dissertation, K.U.Leuven Dept. of Mech. Eng., Leuven, Belgium, 2001.
- [22] K. A. Daltorio, A. D. Horchler, S. Gorb, R. E. Ritzmann, and R. D. Quinn, "A small wall-walking robot with compliant, adhesive feet," in *International Conference on Intelligent Robots and Systems*, 2005, pp. 4018–23.
- [23] P. Cognard, "Collage des matériaux - mécanismes. classification des colles," in *Techniques de l'ingénieur*, 2002.
- [24] A. K. Geim, S. Dubonos, I. V. Grigorieva, K. S. Novoselov, A. A. Zhukov, and S. Y. Shapoval, "Microfabricated adhesive mimicking gecko foot-hair," *Nature Materials*, vol. 2, pp. 461–463, June 2003.
- [25] B. Eyglument, *Manuel de thermique : théorie et pratique*, 2nd ed. Hermes, 1997.
- [26] M. N. Ozisik, *Finite difference methods in heat transfert*. CRC Press, 1994.
- [27] C. Clévy, A. Hubert, and N. Chaillet, "Modeling, identification and control of a thermal glue based temporary fixing system: application to the microrobotic field," in *International Conference on Robotic and Automation*, May 2006.
- [28] C. Clévy, A. Hubert, J. Agnus, and N. Chaillet, "A micromanipulation cell including a tool changer," *Journal of Micromechanics and Micro-engineering*, vol. 15, pp. 292–301, September 2005.
- [29] C. Clévy, A. Hubert, S. Fahlbusch, N. Chaillet, and J. Michler, "Design, fabrication and characterization of a flexible system based on thermal glue for in air and in sem microassembly," in *EFAC International Precision Assembly Seminar*, Bad Hofgastein, Austria, February 2006, pp. 21–31.
- [30] Y. Shen, N. Xi, U. C. Wejinya, and W. J. Li, "High sensitive 2-d force sensor for assembly of surface mems devices," in *International Conference on Intelligent Robots and Systems*, Sendai, Japan, September 2004, pp. 3363–3368.
- [31] C. K. M. Fung, I. Elhaji, W. J. Li, and N. Xi, "A 2-d pvdf force sensing system for micro-manipulation and micro-assembly," in *International Conference on Robotics and Automation*, Washington DC, USA, May 2002, pp. 1489–94.
- [32] Y. Yamamoto, R. Konishi, Y. Negishi, and T. Kawakami, "Prototyping ubiquitous micro-manipulation system," in *International Conference on Advanced Mechatronics*, 2003, pp. 709–714.
- [33] S. Fatikow, J. Seyfried, S. Fahlbusch, A. Buerkle, and F. Schmoedel, "A flexible microrobot-based microassembly station," *Journal of Intelligent and Robotic Systems*, vol. 27, no. 1-2, pp. 135 – 169, January 2000.
- [34] G. Yang, J. A. Gaines, and B. J. Nelson, "A flexible experimental workcell for efficient and reliable wafer-level 3d microassembly," in *International Conference on Robotics and Automation*, Seoul, Korea, May 2001, pp. 133–138.
- [35] W. H. Lee, B. H. Kang, Y. S. Oh, H. Stephanou, A. C. Sanderson, G. Skidmore, and M. Ellis, "Micropeg manipulation with compliant microgripper," in *International Conference on Robotics and Automation*, Tapei, Japan, 2003, pp. 3213–3218.
- [36] N. Dechev, W. L. Cleghorn, and J. K. Mills, "Microassembly of 3-d microstructures using a compliant, passive microgripper," *Journal of Microelectromechanical Systems*, vol. 13, no. 2, pp. 176–189, April 2004.
- [37] D. O. Popa and H. E. Stephanou, "Micro and meso scale robotic assembly," *SME Journal of Manufacturing Processes*, vol. 6, no. 1, pp. 52–71, 2004.
- [38] K. B. Choi, S. H. Kim, and B. W. Choi, "Moving-magnet type precision miniature platform for fine positioning and compliant motion," *Mechatronics*, vol. 11, pp. 921–937, 2001.